第 30 卷第 2 期
2014 年 2 月

无 机 化 学 学 报
CHINESE JOURNAL OF INORGANIC CHEMISTRY

Vol.30 No.2
411-418

基于 π···π 和 C–H···π 作用力构筑的磺酰腙镍(Ⅱ)配合物的超分子组装

王璟琳[1] 焦 勇[2] 杨斌盛*,[2]

([1]长治学院化学系,长治 046011)

([2]山西大学分子科学研究所,太原 030006)

摘要:在温和条件下,以对甲苯磺酰氯为初始原料合成了具有新颖 Ni-O(磺酰基)配键的磺酰腙镍(Ⅱ)配合物 NiL_2(HL:4-甲基-*N*′-(吡啶-2-亚甲基)苯磺酰肼)。晶体结构研究表明,该配合物仅通过 π···π 和 C–H···π 作用组装成两种不同类型的二聚体,一是通过平行四重芳基环绕(P4AE:由面对面(OFF)和边对面(EF)π 堆积组成)相互作用组装而成,二是仅通过 OFF 相互作用进行组装。沿着 *c* 轴方向,两类二聚体通过 P4AE 和 OFF 作用的组合,以“头碰头”形式组装成一维链。每个二聚体均包含了两种不同的对映体形式。利用 B3LYP/6-31++G** 方法,对两种二聚体结构单元单点能计算表明,具有 P4AE 作用的二聚体存在着 OFF 和 EF 的协同作用,也印证和和支持了实验结果。光谱研究确证溶液中 Ni(Ⅱ)和 HL 形成了物质的量之比为 1:2 配合物。

关键词:磺酰腙镍(Ⅱ)配合物;晶体结构;π···π 相互作用;B3LYP/6-31++G** 方法

中图分类号:O614.81+3 **文献标识码**:A **文章编号**:1001-4861(2014)02-0411-08

DOI:10.11862/CJIC.2014.030

Supramolecule Assembled from Sulfonyl Hydrazone Ni(Ⅱ) Complex via π···π and C–H···π Interactions

WANG Jing-Lin[1] JIAO Yong[2] YANG Bin-Sheng*,[2]

([1]*Department of Chemistry, Changzhi University, Changzhi, Shanxi* 046011, *China*)

([2]*Key Laboratory of Chemical Biology and Molecular Engineering of the Ministry of Education, Institute of Molecular Science, Shanxi University, Taiyuan* 030006, *China*)

Abstract: An intriguing supramolecular complex NiL_2 (HL: (*E*)-4-methyl-*N*′-(pyridin-2-ylmethylene) benzenesulfonohydrazide) with novel Ni-O (sulfonyl) coordination bond has been synthesized and characterized. The structural studies indicate that two types of dimers are assembled via intermolecular offset face-to-face π···π stacking (OFF) and edge-to-face C–H···π (EF) interactions between two pyridyl rings in the crystal structure of NiL_2. Each dimer exists in two enantiomeric forms. The DFT calculation indicates that the parallel fourfold aryl embrace (P4AE) interactions, with one OFF interaction and two EF interactions, are stronger than that of only OFF, which can be called synergistic effects. The spectral studies show that the ratio of Ni(Ⅱ) to HL is 1:2 in this compound. CCDC: 773667.

Key words: sulfonyl hydrazone; Ni(Ⅱ) complex; crystal structure; π···π interaction; DFT calculation

收稿日期:2013-04-24。收修改稿日期:2013-07-28。

国家自然科学基金(No.20771068)资助项目。

*通讯联系人。E-mail:yangbs@sxu.edu.cn

In the past decade, supramolecular chemistry is one of the most popular and fastest growing areas of experimental chemistry and it seems set to remain that way for the foreseeable future[1-3]. Although self-assemblies directed by coordination-driven and conventional hydrogen-bonding form high-symmetry conglomerates, other non-covalent interactions such as aromatic π stacking also play an important role in the folding of biological macromolecules and in packing of organic small molecules in crystals. The non-covalent interactions are also used in crystal engineering for the design of functional materials[4-8]. However, it is still a great challenging subject to construct supramolecular polyhedra merely via weaker affinities such as aromatic-aromatic interaction because of the weak attraction of an individual interaction [9]. In this regard, multiple concerted $\pi \cdots \pi$ and C –H $\cdots \pi$ interactions will be required, thus resulting in a collective contribution to the formation of a reliable supramolecular synthon, which has been described as a multiple aryl embrace[10-15].

In this work, the (*E*)-4-methyl-*N*′-(pyridin-2-ylmethylene) benzenesulfonohydrazide (HL) was chosen as the ligand, which is composed of tolyl, pyridyl and sulfonyl hydrazone group, and has the following features: (i) HL is a flexible ligand, and the pyridyl ring connects with tolyl through sulfonyl hydrazone group (-O_2S-NH-N=CH-). It contains N-N, C-C, S-N and S-C single bonds, which can freely rotate according to the demand of coordination, making HL a potential tridentate chelating ligand (Scheme 1). (ii) When deprotonation of the -NH-group, the keto form HL transforms into anionic enolate form L^- resulting in new coordinative properties in metal complex (Scheme 1). For instance, the O atom of sulfonyl and metal Ni(Ⅱ) can form strong coordination bond, which is rarely found in the literature. (iii) HL contains pyridyl ring, yet, in principle, this should be well suited for $\pi \cdots \pi$ interactions because of low π-electron density resulting from nitrogen heteroatoms, which serve as electron acceptors within the ring[16]. (iv) HL is an asymmetrical ligand with a tendency to form chiral

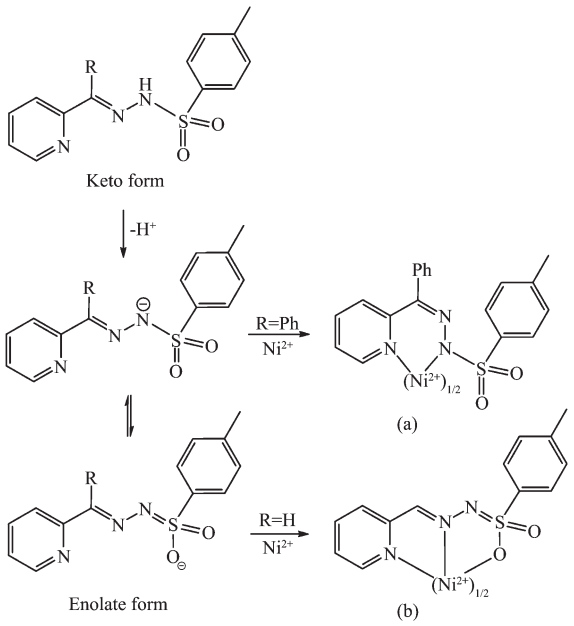

Scheme 1 Keto form, enolate form isomers of ligand and bonding mode of Ni(Ⅱ)-complexes

complexes, in which the only asymmetric center is metal itself[17].

When R=phenyl (Ph), ligand and metal Ni(Ⅱ) can form complex Ni(BPSH)$_2$·H_2O (BPSH=benzoyl pyridin-toluensulfonylhydrazido) [18] which has a distorted tetrahedral structure with two six-membered chelate rings (Scheme 1a). In our work, however, the complex NiL_2 has a distorted octahedral structure with four five-membered chelate rings (Scheme 1b, R=H).

In this paper, we reported synthesis, crystal structure, and DFT calculation together with spectra properties of bis((*E*)-4-methyl-*N*′-(pyridin-2-ylmethylene)phenylsulfohydrazonooxy)Ni(Ⅱ).

1 Experimental

1.1 Materials and general methods

All solvents and starting materials for the synthesis were purchased commercially and were used as received without further purification. Infrared spectra were obtained from KBr pellets on a Shimadzu FTIR-8400S spectrometer in the 400 ~4 000 cm^{-1} region. Elemental analyses (C, H and N) were performed on a Perkin-Elmer 240C elemental analyzer. Absorbance spectra were recorded on a Hewlett_Packard HP-8453 UV-Vis spectrophotometer. The fluorescence emission spectra were recorded on a Cary

Eclipse fluorescence spectrophotometer (Varian). ^{1}H NMR spectra were measured on a Bruker DRX-300 spectrometer in dimethyl sulfoxide DMSO-d_6 solution, with tetramethylsilane (TMS) as the internal standard. The synthetic route of the complexes was shown in Scheme 2.

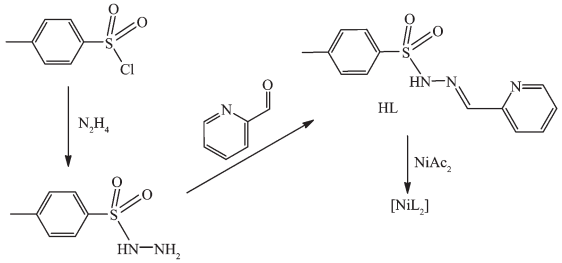

Scheme 2　Synthetic route of the complexes

1.2　Synthesis of 4-methylbenzenesulfonohydrazide

The precursor 4-methylbenzenesulfonohydrazide was synthesized according to literature procedures[19].

1.3　Synthesis of (*E*)-4-methyl-*N*′-(pyridin-2-ylmethylene)benzene sulfonohydrazide (HL)

4-methylbenzenesulfonohydrazide (0.93 g, 5 mmol) was dissolved in MeOH (50 mL). Pyridine-2-aldehyd (500 μL, 5 mmol) was added to the above solution, and the mixture was stirred at room temperature. The white precipitate was formed in solution, and the mixture was further stirred at room temperature for 1.5 h. The precipitate was collected and washed three times with MeOH. Recrystallization from hot MeOH and drying in vacuum afforded a white solid. Yield was 0.75 g (55%). Anal. Calcd. for $C_{13}H_{13}N_3O_2S$(%): C 56.71, H 4.76, N 15.26; Found(%): C 56.63, H 4.75, N 15.31. IR (KBr, cm^{-1}): ν(N-H) 3 053, ν(ArC-H) 2 995, ν(MeC-H) 2 875, ν(C=N) 1 593, ν(SO2) 1 330, 1184, 1 167, ν(S-N) 1 068。^{1}H NMR (300 MHz, DMSO-d_6, δ, ppm): 11.79 (s, 1H), 8.55 (d, J=3.6 Hz, 1H), 7.91 (s, 1H), 7.84 (d, J=7.5 Hz, 1H), 7.81 (d, J=11.4 Hz, 1H), 7.78 (dd, J=8.4 Hz, J=9.9 Hz, 1H), 7.72 (d, J=6.4 Hz, 1H), 7.42 (dd, J=7.8 Hz, J=7.5 Hz, 1H), 7.38 (d, J=5.7 Hz, 1H), 7.36 (d, J=5.4 Hz, 1H), 3.33 (s, 3H).

1.4　Synthesis of bis((*E*)-4-methyl-*N*′-(pyridin-2-ylmethylene) phenylsulfohydrazonooxy) Ni(Ⅱ)

(*E*)-4-methyl-*N*′-(pyridin-2-ylmethylene)benzenesulfonohydrazide (HL) (0.275 g, 1 mmol) was dissolved in 30 mL MeOH and heated to reflux. $Ni(Ac)_2\cdot 4H_2O$ (0.125 g, 0.5 mmol) was then added to the refluxing mixture and further refluxed for 3 h. The reaction mixture was cooled and was placed at room temperature overnight. The brown precipitate was collected and washed three times with MeOH. Yield was 85%. The powdered solid (NiL_2) was dissolved in MeOH, and the single crystals was collected after slow evaporation at room temperature for about several weeks. Anal. Calcd. for $C_{26}H_{24}N_6NiO_4S_2$ (%): C 51.42, H 3.98, N 13.84; Found(%): C 51.34, H 3.98, N 13.91. IR (KBr, cm^{-1}): ν(ArC-H) 3 026, ν(MeC-H) 2 921, ν(C=N) 1 600, ν(SO_2) 1 257, 1 128, 1 105, ν(S-N) 1 047.

1.5　X-ray crystallography

Crystallographic data were collected on a Bruker Smart CCD diffractometer at 298 K using graphite monochromated Mo $K\alpha$ radiation source (λ=0.071 073 nm). Intensity data were corrected for Lorentz and polarization effects. The frames were integrated with the Bruker SAINT[20] software package and the data were corrected for absorption using the program SADABS[21]. The structures were solved by direct methods with SHELXS and refined by full-matrix least-squares analysis with SHELXL-97[22]. All non-H atoms were refined anisotropically with the hydrogen atoms added to their geometrically ideal positions and refined isotropically. Images were created with the SHELXTL and DIAMOND programs[23]. Hydrogen bonding and π-stacking interactions in the crystal lattice were calculated with SHELXTL and DIAMOND programs. Selected crystallographic data and structural determination parameters of complex were given in Table 1.

CCDC: 773667.

1.6　DFT calculation

The calculations were constrained by the data of the bond lengths and the angles, which were taken from the X-ray structure of the NiL_2. The single point energy calculations of two types of dimers $[NiL_2]_2$ were performed at B3LYP/6-31 ++G** basis set level. All calculations were done using the Gaussian03 program[24].

Table 1 Crystallographic Data for NiL_2

Formula	$C_{26}H_{24}N_6NiO_4S_2$	D_c / (g·cm^{-3})	1.498
Formula weight	607.34	Absorption coefficient / mm^{-1}	0.92
Crystal system	Triclinic	F(000)	628
Space group	$P\bar{1}$	Crystal size / mm	0.46×0.30×0.25
a / nm	0.987 7(1)	θ range / (°)	1.66~25.02
b / nm	1.111 7(1)	Reflections collected	7 052
c / nm	1.301 2(2)	Independent reflections (R_{int})	4 679(0.018 3)
α / (°)	108.952(2)	Max. and min. transmission	0.802 6, 0.676 9
β / (°)	93.837(1)	Data, restraints, parameters	4679, 0, 354
γ / (°)	91.298(1)	Goodness-of-fit	1.03
V / nm^3	1.346 8(3)	R factor ($I>2\sigma(I)$)	R_1=0.035 0, wR_2=0.080 0
Z	2	R factor (all data)	R_1=0.051 5, wR_2=0.090 7

2 Results and discussion

2.1 Crystal structure of NiL_2

The single-crystal X-ray diffraction of NiL_2 reveals that it crystallizes in the triclinic space group $P\bar{1}$. The molecular structure of NiL_2 consists of a neutral noncentrosymmetric complex (Fig.1a), that each nickel ion is octahedrally coordinated by two mono-negative tridentate ligands (L^-), and the coordination sphere is occupied by a N_4O_2 donor set from the two ligand units. The Ni-N and Ni-O distances are in the range of 0.200 6(2)~0.207 1(2) nm and 0.213 8(2)

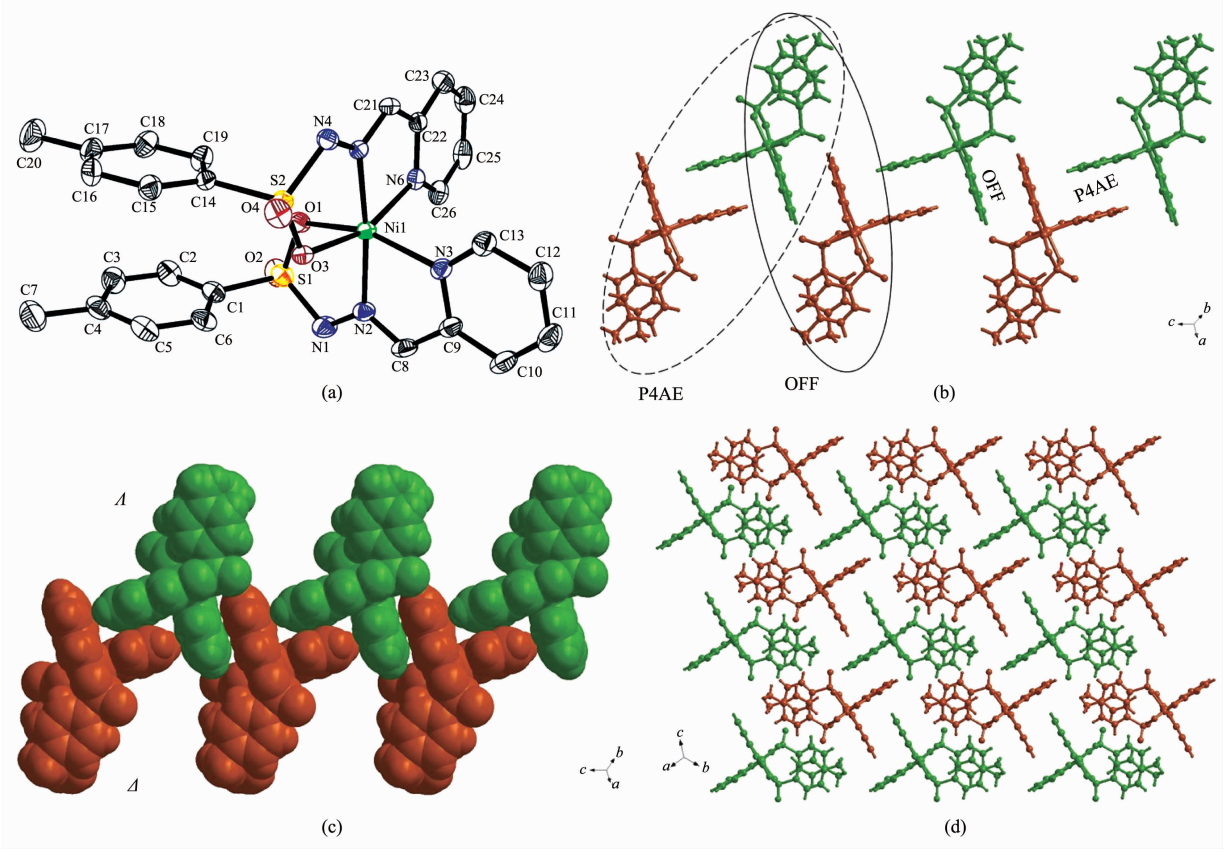

(a) Displacement ellipsoids are drawn at the 30% probability level; For clarity, H atoms have been omitted

Fig.1 (a) Molecular structure of NiL_2 showing the atom-labelling scheme; (b) One-dimensional structure of NiL_2 was formed by P4AE and OFF interactions and extending along the c axis; (c) Space-filling model of π-stacking interactions; (d) Arrangement of one-dimensional chains in the (110) plane

Table 2　Selected bond lengths (nm) and bond angles (°) for NiL_2

Ni(1)-N(5)	0.200 6(2)	Ni(1)-O(3)	0.213 8(2)	O(3)-S(2)	0.147 0(2)
Ni(1)-N(2)	0.201 4(2)	Ni(1)-O(1)	0.214 2(2)	O(4)-S(2)	0.143 1(2)
Ni(1)-N(3)	0.206 4(2)	O(1)-S(1)	0.147 1(2)	Ni(1)-N(6)	0.207 1(2)
O(2)-S(1)	0.143 7(2)				
N(5)-Ni(1)-N(2)	171.88(9)	N(3)-Ni(1)-N(6)	94.34(9)	N(5)-Ni(1)-O(1)	101.13(8)
N(5)-Ni(1)-N(3)	100.51(9)	N(5)-Ni(1)-O(3)	78.78(8)	N(2)-Ni(1)-O(1)	78.42(9)
N(2)-Ni(1)-N(3)	80.50(10)	N(2)-Ni(1)-O(3)	93.14(8)	N(3)-Ni(1)-O(1)	158.22(9)
N(5)-Ni(1)-N(6)	79.95(9)	N(3)-Ni(1)-O(3)	92.56(8)	N(6)-Ni(1)-O(1)	87.05(8)
N(2)-Ni(1)-N(6)	108.07(9)	N(6)-Ni(1)-O(3)	158.50(8)	O(3)-Ni(1)-O(1)	94.00(7)

Table 3　π-stacking interactions existing in the NiL_2

Interaction group	Interaction type	Central separation / nm	Shortest Contact / nm	Angle / (°)[a]
ph-ph	π…π[b]	0.3814	0.3633	θ=17.7
py-py	π…π(OFF)	0.3562	0.3463	θ=13.5
py-py	π…π(P4AE)	0.3613	0.3380	θ=20.7
py-py	C–H…π(P4AE)	0.2806[c]		β=168.5

[a] θ angle between the ring normal and centroid–centroid vector in π-π stacking; β angle of C–H…ring centroid in C–H…π interactions; [b] Intramolecular π…π interactions; [c] Separation of an H atom and π ring centroid.

~0.214 2(2) nm, respectively. The selected bond distances and angles are listed in Table 2.

The most striking feature of the crystal structure is: (i) The O atom of sulfonyl and metal Ni(Ⅱ) can form strong coordination bond, which is rarely found in the literature. The possible reason is strong electron-withdrawing properties of the Ni(Ⅱ) ion reduce the electron density on the coordinated ligand lead to its keto form transforms into mono-negative enolate form, which well-suited for the formation of strong coordination bond. (ii) Chiral recognition observed in the solid state for NiL_2 due to intermolecular π…π and C–H…π interactions between two pyridyl rings (Fig.1b)[25-28]. NiL_2 are octahedral complex in which the only asymmetric center is the metal itself and which thus exists in two enantiomeric forms, named *Λ* and *Δ* (Fig.1b and 1c). Obviously, such complexes are in general prepared as a racemic mixture of the two enantiomers. (iii) The crystal structure of NiL_2 exhibits various self-assembly process by intra- and intermolecular π…π interactions. As shown in Fig.1b, not only intramolecular π…π interactions exist in NiL_2, but also intermolecular π…π interactions exist. The neighboring molecules of NiL_2 are assembled in a mutual head-to-head manner by offset face-to-face (OFF) and edge-to-face (EF) interactions to form infinite 1D chain structures along the c axis. One section of Fig. 1b highlighted in black solid lines, showing OFF π…π stacking interactions between pyridyl rings of ligand moieties; the other of Fig.1b highlighted in black dash lines, in one OFF interaction together with two EF interactions, formed the parallel fourfold aryl embrace (P4AE). All of these interaction separations and angles are listed in Table 3.

Fig.1c reveals the space-filling model of P4AE-EF interactions along the *c* axis. Fig.1d shows the self-assembly of one-dimensional chains by weak intermolecular interactions to form the (110) plane.

2.2　DFT calculation based on dimers of NiL_2

As shown in Fig.1b, the NiL_2 is divided into two types of dimers, which contain P4AE and OFF interactions respectively. The single point energy calculations of these dimers are performed at B3LYP/6-31++G** basis set level, and different eigenvalues of correlative HOMOs are compared. Eigenvalues of HOMOs are listed in Table 4. The MOs energy-level diagrammatic drawings of two types of dimers are shown in Fig.2.

Table 4 Eigenvalues (kJ·mol^{-1}) of MOs for two types dimers of NiL_2

MOs	E_{P4AE}	E_{OFF}	$E_{P4AE}-E_{OFF}$
LUMO	−350.110	−333.583	−16.528
HOMO-00	−369.912	−353.106	−16.806
HOMO-01	−369.991	−353.327	−16.664
HOMO-02	−507.785	−496.319	−11.466
HOMO-03	−514.559	−498.417	−16.142
HOMO-04	−520.025	−503.975	−16.050
HOMO-05	−522.236	−505.440	−16.795
HOMO-06	−539.091	−522.876	−16.215
HOMO-07	−541.738	−524.950	−16.787
HOMO-08	−583.951	−569.088	−14.863
HOMO-09	−584.783	−569.642	−15.141
HOMO-10	−585.030	−578.532	−6.498

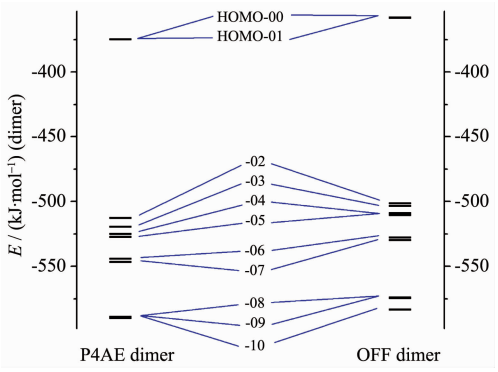

Fig.2 MOs energy-level diagrammatic drawing of two types of dimers with P4AE and OFF interactions respectively

The DFT calculation indicates that P4AEs interactions are stronger than these of OFFs, the corresponding eigenvalues of HOMOs with P4AEs interactions are lower than these of HOMOs with OFFs interactions. It is shown that complex NiL_2 exists as synergistic effects of OFF-$(EF)_2$ interactions. For example, the $E_{P4AE}-E_{OFF}$ of dimers is −16.806 kJ·mol^{-1} for HOMO-00, this stabilization is lower than the intermolecular energy of a pair of benzene molecules, *ca* 9.2 kJ·mol^{-1} [10].

The calculations from dimers, which contain P4AE and OFF interactions, respectively, give the highest occupied molecular orbitals HOMO-00 and HOMO-01 ~HOMO-10. The selected HOMOs are shown in Fig.3. HOMO-5s for P4AE and OFF display the $\pi\cdots\pi$ stacking interactions between the two

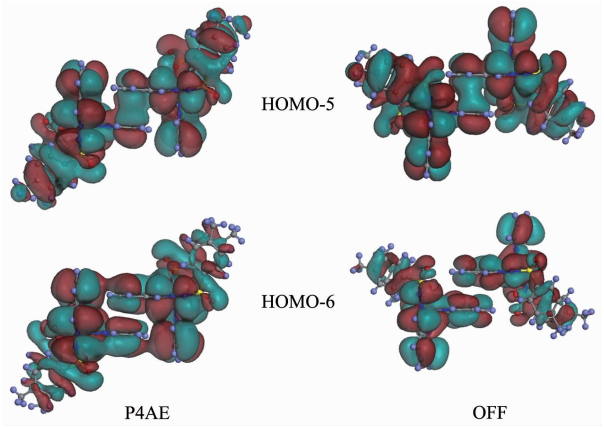

Fig.3 Selected HOMOs of two types of dimers

pyridyl groups. The HOMO-6 for P4AE clearly reveals C−H$\cdots\pi$ interaction; however, HOMO-6 for OFF no C−H$\cdots\pi$ interaction exists.

2.3 Spectra properties of NiL_2

Fig.4 shows the variation of spectra upon addition of sequential aliquots Ni(Ⅱ) to the DMSO solution of HL at 25 ℃. The HL has a strong absorption peak at 287 nm and weak absorption peak at 351 nm, and are attributed to $\pi\rightarrow\pi^*$ and $n\rightarrow\pi^*$ transitions, respectively. Upon the addition of Ni(Ⅱ) (0~1 equiv.), the absorbance at 287 nm decreases and at 351 nm increases (Fig.4), a red shift of each absorption spectrum is observed (from 351 nm red-shifted to 362 nm). It is likely that coordination of the ligand to an electropositive metal stabilizes the HOMO and LUMO to different extents resulting in a smaller

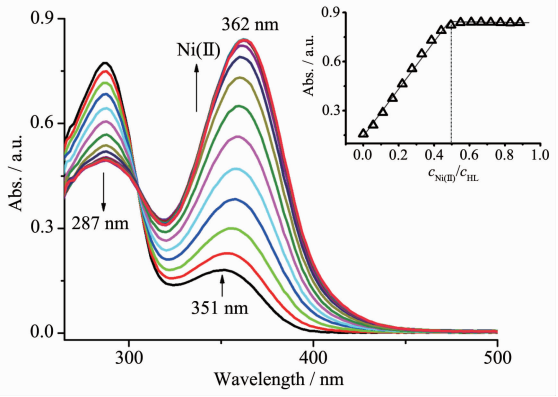

Each successive trace represents the addition of an additional 0.05 equivalent of Ni(Ⅱ); Inset: UV titration curve at 362 nm; c_{HL}=4.0×10^{-5} mol·L^{-1}

Fig.4 Progressive changes in the UV spectra of HL observed upon addition of Ni(Ⅱ) in DMSO at 25 ℃

n-π* energy gap and a lower energy transition. As indicated in Fig.4, all display an isosbestic point, indicating the formation of the UV-active complex. In addition, the saturated spectra are readily obtained when 0.5 equiv of Ni(Ⅱ) ions is introduced to the solution of HL, showing the formation of 1:2 metal/ligand ratio compounds. The UV titration curves of HL with Ni(Ⅱ) ions are also done in DMSO medium at 25 ℃ (Fig.4 Inset). It can be seen that a sharp inflexion appeared at about c_{Ni}/c_{HL}=0.5, which confirmed the 1:2 stoichiometric ratio of Ni(Ⅱ) and HL in the complex.

The electronic spectra in the visible region are observed upon addition of different concentration NiL_2 in DMSO at 25 ℃. The three absorption bands, which are at 362, 530 and 885 nm (Fig.5), are attributed to $^3A_{2g}\rightarrow{}^3T_{1g}$ (*P*), $^3A_{2g}\rightarrow{}^3T_{1g}$ (*F*) and $^3A_{2g}\rightarrow{}^3T_{2g}$ [$(t_{2g}^6e_g^2)\rightarrow(t_{2g}^5e_g^3)$] transitions, respectively.

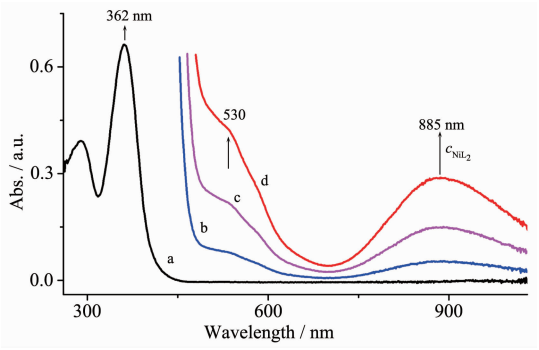

Curve a: $c_{NiL_2}=3\times10^{-5}$ mol·L^{-1}; curve b: $c_{NiL_2}=5\times10^{-4}$ mol·L^{-1}; curve c: $c_{NiL_2}=6\times10^{-3}$ mol·L^{-1}; curve d: $c_{NiL_2}=8\times10^{-2}$ mol·L^{-1}

Fig.5　Absorption spectra of the NiL_2 in DMSO solution at 25 ℃

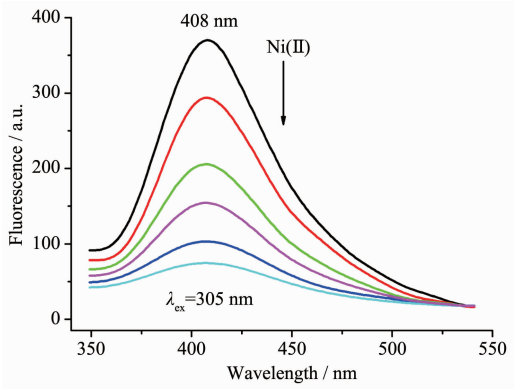

Each successive trace represents the addition of an additional 0.1 equivalent of Ni(Ⅱ), slit width=10 nm, λ_{ex}=305 nm; $c_{HL}=4.0\times10^{-5}$ mol·L^{-1}

Fig.6　Fluorescence emission spectra for the addition of Ni(Ⅱ) to the DMSO solution of HL at 25 ℃

The addition of sequential aliquots of Ni(Ⅱ) to DMSO solution of HL produce fluorescence spectra, as shown in Fig.6. Maximal emission bands appear at 408 nm, and fluorescence quenching are observed by the addition of Ni(Ⅱ). The mechanisms for quenching are expected to electron exchange or photoinduced electron transfer or combination of these mechanisms[29].

3　Conclusions

The tridentated (NNO) ligand HL and its Ni(Ⅱ) complex have been prepared, and are characterized by X-ray crystallography, IR and ^{1}H NMR spectroscopy, and elemental analyses. The interactions between Ni(Ⅱ) and HL are also investigated by using absorption spectra and fluorescence spectra. From these studies, the following conclusions are derived: (i) The ligand HL coordinated to Ni(Ⅱ) in mono-negative enolate form, and one of O atoms in sulfonyl and metal Ni(Ⅱ) can form strong coordination bond. (ii) Chiral recognition is observed in the crystal structure of NiL_2 merely via intermolecular π … π and C –H … π interactions between two pyridyl rings. And the neighboring molecules of NiL_2 are arranged in a mutual head-to-head manner by OFF and EF interactions to form infinite 1D chain structures along the *c* axis. (iii) The DFT calculation indicates that P4AEs interactions are stronger than those of OFFs, and exist as synergistic effects of EF-OFF interactions in NiL_2. (iv) UV-Vis and fluorescence spectral studies show that Ni(Ⅱ)/HL ratio is 1:2 in Ni(Ⅱ)-L complex.

References:

[1] Steed J W, Atwood J L. *Supramolecular Chemistry*. 2*nd Ed*. Chichester: John Wiley & Sons, Ltd., **2009**:2-9

[2] Leininger S, Olenyuk B, Stang P J. *Chem. Rev.*, **2000**,**100**: 853-908

[3] LI Zheng(李正), ZHAO Yue(赵越), WANG Peng(王鹏), et al. *Chinese J. Inorg. Chem.*(无机化学学报), **2012**,**28**(7): 1469-1476

[4] Huang W, Zhu H B, Gou S H. *Coord. Chem. Rev.*, **2006**, **250**:414-423

[5] Tiefenbacher K, Rebek Jr J. *J. Am. Chem. Soc.*, **2012**,**134**:

2914-2017

[6] Desiraju G R. *Angew. Chem. Int. Engl.*, **1995**,**34**:2311-2327

[7] NI Zhong-Hai(倪中海), NIE Jing(聂景), LI Guo-Ling(李国玲), et al. *Chinese J. Inorg. Chem.*(无机化学学报), **2012**, **28**(2):411-416

[8] Quiñonero D, Frontera A, Escudero D, et al. *Theor. Chem. Account*, **2008**,**120**:385-393

[9] Wei W, Wu M, Gao Q, et al. *Inorg. Chem.*, **2009**,**48**:420-422

[10]Dance I, Scudder M. *CrystEngComm*, **2009**,**11**:2233-2247

[11]Russell V, Scudder M, Dance I. *J. Chem. Soc., Dalton Trans.*, **2001**:789-799

[12]McMurtrie J, Dance I. *CrystEngComm*, **2005**,**7**:216-229

[13]Dance I. *New J. Chem.*, **2003**,**27**:22-27

[14]Dance I. *CrystEngComm*, **2003**,**5**:208-221

[15]Lacour J, Bernardinelli G, Russell V, et al. *CrystEngComm*, **2002**,**4**(30):165-170

[16]Janiak C. *J. Chem. Soc., Dalton Trans.*, **2000**:3885-3896

[17]Wang J, Liu B, Yang B. *CrystEngComm*, **2011**,**13**:7086-7097

[18]Döring M, Görls H, Uhlig E. *Z. Anorg. Allg. Chem.*, **1992**, **613**:55-59

[19]Larabi L, Harek Y, Reguig A, et al. *J. Serb. Chem. Soc.*, **2003**,**68**(2):85-95

[20](a)*SMART* (*control*) *and SAINT* (*integration*) *Software*, *Bruker Analytical X-ray Systems*, Madison, WI, **1994**.

(b)*Bruker*, *SMART*(*Version* 5.0) *and SAINT* (*Version* 6.02), Bruker AXS Inc., Madison, Wisconsin, USA, **2000**.

[21]Sheldrick G M. *SADABS*, *A Program for Absorption Corrections*, University of Göttingen, Germany, **1996**.

[22]Sheldrick G M. *SHELXL*97, *A Program for the Refinement of Crystal Structures from X-ray Data*, University of Göttingen, Germany, **1997**.

[23]Klaus B. *DIAMOND*, *Version* 1.2*c*, University of Bonn, Germany, **1999**.

[24]Frisch M J, Trucks G W, Schlegel H B, et al. *Gaussian* 03, Gaussian Inc., Pittsburgh, PA, **2003**.

[25]Chavarot M, Ménage S, Hamelin O, et al. *Inorg. Chem.*, **2003**,**42**:4810-4816

[26]Li M, Sun Q, Bai Y, et al. *Dalton Trans.*, **2006**:2572-2578

[27]Zuccaccia D, Bellachioma G, Cardaci G, et al. *Dalton Trans.*, **2006**:1963-1971

[28]Gao E Q, Yue Y F, Bai S Q, et al. *J. Am. Chem. Soc.*, **2004**,**126**:1419-1429

[29]Lakowicz J R. *Principles of Fluorescence Spectroscopy*. 3*rd. Ed*. New York: Springer Science +Business Media, LLC, **2006**:334-338